2024 IEEE 63rd Conference on Decision and Control (CDC)
December 16-19, 2024. MiCo, Milan, Italy

Fully Distributed EV Charging Scheduling for Load Flattening in V2G Systems

Jinwook Heo[1], Soojeong Hyeon[1], Hyungbo Shim[1,*], and Jinsung Kim[2]

Abstract— **This paper presents a fully distributed algorithm for scheduling electric vehicle (EV) charging and discharging to flatten the total load of the grid, while considering constraints on grid transmission capacity. As a fully distributed solution, the proposed algorithm operates without the need for a central unit. Instead, each agent only communicates a single dual variable with its neighboring agents based on a communication graph, and thus no private information is shared. In particular, the algorithm does not rely on initial conditions, ensuring robustness in online changes of operational conditions. Simulation results verify the effectiveness of the proposed algorithm.**

I. Introduction

The advent of vehicle-to-grid (V2G) technology enables electric vehicles (EVs) to serve as controllable loads and distributed energy resources within the power grid. V2G facilitates a bidirectional exchange of electricity between EVs and the grid, positioning EVs as key components in managing intermittent renewable energy sources like wind and solar power [1]. As the EV population grows, their charging and discharging behavior significantly impacts grid operations, making effective scheduling essential for maintaining grid stability and preventing load peaks. This strategy could minimize operational costs, enhance system efficiency, and benefit EV users [2].

This paper focuses on EV scheduling to flatten the grid's load profile. We also consider battery degradation for each EV user, as frequent charging and discharging can reduce battery lifespan. Furthermore, grid capacity constraints are considered to prevent overloading of transmission lines. Roughly speaking, load flattening aims to evenly spread power consumption over a given time horizon T. The main objective is to minimize the function represented by

$$\sum_{k=0}^{T-1}\left(D[k]+\sum_{i=1}^{N}u_i[k]\right)^2 \tag{1}$$

where $u_i[k] \in \mathbb{R}$ represents a charging and discharging power for each EV $i \in \{1,2,\dots,N\}$ at a time slot $k \in \{0,1,\dots,T-1\}$, and $D[k]$ denotes a forecasted base load of the grid at time slot k. Note that the objective function (1) does not directly decompose into individual functions for each agent i, and the considerations of grid transmission yield global coupling constraints among agents.

Centralized algorithms for solving this problem encounter challenges as the number of EVs increases, including privacy concerns and computational overhead on a central infrastructure [3]. For this reason, distributed methods [4], [5] have been developed to alleviate these burdens by enabling EVs to optimize their charging schedules in response to an external price signal from the center known as an aggregator. Specifically, in [4], a dual-splitting method is introduced to decompose the coupled variables in the objective (1) to parallelize the optimization problem. However, since they still need the center, we categorize them as "semi-distributed" in this paper. Unfortunately, this framework continues to suffer from computational burdens and privacy concerns.

Meanwhile, fully distributed algorithms [6], [7] have been introduced to tackle constraint-coupled optimization problems, addressing the difficulty of handling global constraints without the central unit. However, they require a specific initialization process, which leads to another challenge when agents join or leave the network during the operation, therefore, the *plug-and-play operation* is not guaranteed. In particular, the states of all remaining agents in the network must be re-initialized for each change in operational condition, which is difficult to achieve in a fully distributed manner. Consequently, these algorithms have limitations in addressing the dynamic nature of EV arrivals and departures in real-world applications.

In this paper, we propose a fully distributed continuous-time algorithm based on the blended dynamics approach [8]–[11] for load flattening while satisfying grid constraints. Notably, the algorithm is initialization-free, ensuring resilience to real-time changes in grid constraints or network topology. Moreover, it is center-free and preserves privacy, as each agent exchanges only a single dual variable with its neighbors, rather than each EV being directly connected to the aggregator. In our framework, the aggregator is treated as one of the agents within a communication network and holds global information, such as grid constraints. This allows for a decentralized design where newly participating EVs can design their dynamics using only local information.

The remaining sections are organized as follows. Section II introduces the problem formulation and a semi-distributed solution is presented in Section III. Section IV introduces the blended dynamics theorem and proposes a fully distributed algorithm. Simulation results are shown in Section V and the paper concludes in Section VI.

Notation: We let 0_n and 1_n be the $n \times 1$ column vectors

*This work was supported by the grant from Hyundai Motor Company's R&D Division.

[1]ASRI, Department of Electrical and Computer Engineering, Seoul National University, Seoul, 08826, Korea. jwheo, hsj9537@cdsl.kr, hshim@snu.ac.kr

*Corresponding author.

[2]Vehicle SW Division, Hyundai Motor Company, Hwaseong, 18280, Korea. jinsung.kim@hyundai.com

consisting of all zeros and ones, respectively, and denote the $n \times n$ identity matrix by I_n. For given vectors or matrices a and b, we denote $[a^\top, b^\top]^\top$ by $[a; b]$. For a vector x and a matrix A, $\|x\|$ and $\|A\|$ denote the Euclidean norm and the induced matrix 2-norm, respectively. The operation defined by the symbol $\otimes$ is the Kronecker product. Let $\mathbb{R}_+^n$ denote nonnegative real vector space. For a vector $x = [x_1; \ldots; x_n] \in \mathbb{R}^n$, $(x)^+ = [\max(0, x_1); \ldots; \max(0, x_n)] \in \mathbb{R}_+^n$. For a set $\Xi \subset \mathbb{R}^n$, $\|x\|_\Xi$ denotes the distance between the vector $x \in \mathbb{R}^n$ and Ξ; i.e., $\|x\|_\Xi := \inf_{y \in \Xi} \|x - y\|$.

II. Problem Formulation

We consider a situation where a fleet of N vehicles participates in an electricity distribution network. Each EV, denoted by $i \in \mathcal{N} := \{1, \ldots, N\}$, has a charging and discharging power $u_i[k] \in \mathbb{R}$ for a given time slot $k \in \mathcal{T} := \{0, \ldots, T-1\}$. This section formulates an optimization problem for load flattening and provides a mathematical representation to design an optimal charging and discharging schedule $u_i := [u_i[0]; \ldots; u_i[T-1]] \in \mathbb{R}^T$.

A. Constraints

1) Local Constraints: Let $e_i[k]$ represent the battery energy level of EV i at time slot k, and ΔT denote the duration of time intervals. The local constraints for each EV i are expressed as follows:

$$U_i^{\min} \le u_i[k] \le U_i^{\max} \tag{2a}$$
$$e_i[0] = E_i^{\text{init}} \tag{2b}$$
$$e_i[k+1] = e_i[k] + \Delta T u_i[k] \tag{2c}$$
$$e_i[T] \ge E_i^{\text{ref}} \tag{2d}$$
$$E_i^{\min} \le e_i[k] \le E_i^{\max} \tag{2e}$$

where $U_i^{\max} \ge 0$ and $U_i^{\min} \le 0$ are the bounds on charging and discharging power; E_i^{init} and E_i^{ref} represent the initial and reference energy, respectively; $E_i^{\min}$ and $E_i^{\max}$ are the battery energy capacity limits.

The constraints (2a)–(2e) can be simplified into the following matrix forms, solely in terms of charging and discharging schedule u_i. From (2a), we have

$$\underline{U}_i \le u_i \le \overline{U}_i \tag{3}$$

where $\underline{U}_i = [U_i^{\min}; \ldots; U_i^{\min}]$, $\overline{U}_i = [U_i^{\max}; \ldots; U_i^{\max}]$, and the inequalities between vectors are understood in a component-wise sense. Furthermore, considering (2c) for all time slot $k \in \mathcal{T}$, equations (2b)–(2e) can be expressed as

$$\begin{aligned} E_i^{\min} \le{} & E_i^{\text{init}} + \Delta T u_i[0] \le E_i^{\max} \\ E_i^{\min} \le{} & E_i^{\text{init}} + \Delta T \left(u_i[0] + u_i[1]\right) \le E_i^{\max} \\ & \vdots \\ E_i^{\text{ref}} \le{} & E_i^{\text{init}} + \Delta T \sum_{k=0}^{T-1} u_i[k] \le E_i^{\max} \end{aligned}$$

resulting in the following matrix representation:

$$\underline{E}_i \le L u_i \le \overline{E}_i \tag{4}$$

where

$$L = \Delta T \begin{bmatrix} 1 & 0 & \cdots & 0 \\ 1 & 1 & \cdots & 0 \\ \vdots & \vdots & \ddots & \vdots \\ 1 & 1 & \cdots & 1 \end{bmatrix} \in \mathbb{R}^{T \times T},$$

$$\underline{E}_i = \begin{bmatrix} -E_i^{\text{init}} + E_i^{\min} \\ \vdots \\ -E_i^{\text{init}} + E_i^{\min} \\ -E_i^{\text{init}} + E_i^{\text{ref}} \end{bmatrix}, \quad \overline{E}_i = \begin{bmatrix} -E_i^{\text{init}} + E_i^{\max} \\ \vdots \\ -E_i^{\text{init}} + E_i^{\max} \\ -E_i^{\text{init}} + E_i^{\max} \end{bmatrix}.$$

2) Global Constraints: There are limits on the total delivery power for the grid to avoid congestion. Therefore, the aggregate charging and discharging power of EVs should be bounded within the grid capacity limits, as given by

$$\underline{P} \le \sum_{i=1}^{N} u_i \le \overline{P} \tag{5}$$

where $\underline{P} = [P^{\min}; \ldots; P^{\min}]$ and $\overline{P} = [P^{\max}; \ldots; P^{\max}]$.

B. Objective

The objective is to flatten the total load of the grid considering prevention of battery degradation for each EV user. We denote a forecasted base load by $D = [D[0]; \ldots; D[T-1]]$. Then, the overall optimization problem with constraints (3), (4), and (5) is formulated as follows:

$$\min_u \; J(u) = \sum_{k=0}^{T-1} \left(D[k] + \sum_{i=1}^{N} u_i[k] \right)^2 + \sum_{i=1}^{N} \sigma_i \|u_i\|^2 \tag{6a}$$
$$\text{s.t.} \; \underline{P} \le \sum_{i=1}^{N} u_i \le \overline{P} \tag{6b}$$
$$A u_i \le b_i, \quad i \in \mathcal{N} \tag{6c}$$

where $u = [u_1; \ldots; u_N] \in \mathbb{R}^{NT}$. Here, the matrices $A := [-I_T; I_T; -L; L] \in \mathbb{R}^{4T \times T}$ and $b_i := [-\underline{U}_i; \overline{U}_i; -\underline{E}_i; \overline{E}_i] \in \mathbb{R}^{4T}$ are obtained from the constraints (3) and (4).

The first term in the objective function $J(u)$ reflects the variance of the total load over the time horizon T, indicating the extent of fluctuations in the load profile. The second term represents the battery degradation cost, including a degradation parameter σ_i selected by each EV user. This term addresses the impact of charging and discharging power on battery degradation, using a simplified model in this paper.

III. A Semi-Distributed Solution

In this section, we introduce a semi-distributed solution to solve the problem (6), serving as the foundation for a fully distributed one will be discussed in Section IV. We develop a dual-splitting method specifically tailored from the result of [4] to handle coupled variables within the objective function (6a) and to address the global constraints (6b).

To begin, let us define a new variable $z[k] = D[k] + \sum_{i=1}^{N} u_i[k]$ for $k \in \mathcal{T}$, and let $z = [z[0]; \ldots; z[T-1]]$.

Accordingly, we modify the constraints (6b) to $D + \underline{P} \le z \le D + \overline{P}$. Then, the problem (6) can be rewritten as

$$\min_{z,\,u} \;\|z\|^2 + \sum_{i=1}^{N} \sigma_i \|u_i\|^2 \tag{7a}$$
$$\text{s.t.}\;\; z = D + \textstyle\sum_{i=1}^{N} u_i \tag{7b}$$
$$D + \underline{P} \le z \le D + \overline{P} \tag{7c}$$
$$Au_i \le b_i, \quad i \in \mathcal{N}. \tag{7d}$$

Define the feasible sets as $\mathcal{Z} := \{z \in \mathbb{R}^T : D + \underline{P} \le z \le D + \overline{P}\}$, $\mathcal{U}_i := \{u_i \in \mathbb{R}^T : Au_i \le b_i\}$, and $\mathcal{U} := \mathcal{U}_1 \times \cdots \times \mathcal{U}_N$. It is noted that if the constraint (7b) is removed, the problem (7) can be separated into subproblems that can be solved independently. By introducing the Lagrange multiplier $\lambda = [\lambda[0]; \dots; \lambda[T-1]]$ for (7b), the dual function $g : \mathbb{R}^T \to \mathbb{R}^T$ is obtained as

$$g(\lambda) = \min_{\substack{z \in \mathcal{Z} \\ u \in \mathcal{U}}} \|z\|^2 + \lambda^\top \left(D + \sum_{i=1}^{N} u_i - z \right) + \sum_{i=1}^{N} \sigma_i \|u_i\|^2$$
$$= \min_{z \in \mathcal{Z}} \left(\|z\|^2 + \lambda^\top (D - z) \right) + \sum_{i=1}^{N} \min_{u_i \in \mathcal{U}_i} \left(\sigma_i \|u_i\|^2 + \lambda^\top u_i \right)$$

which clearly decouples into separate minimization subproblems with respect to the variables z and u_i.

Now, we express the first term in $g(\lambda)$ as the sum of T minimization problems for $z[k]$ and obtain its explicit form as follows:

$$\sum_{k=0}^{T-1} \begin{pmatrix} \min_{z[k]} \; (z[k])^2 - \lambda[k] z[k] + \lambda[k] D[k] \\ \text{s.t. } D[k] + P^{\min} \le z[k] \le D[k] + P^{\max} \end{pmatrix}$$
$$= \sum_{k=0}^{T-1} \left((\theta_k(\lambda[k]))^2 - \lambda[k]\theta_k(\lambda[k]) + \lambda[k] D[k] \right) =: \Theta(\lambda)$$

where $\theta_k(\lambda[k]) : \mathbb{R} \to \mathbb{R}$ is the closed-form solution of the quadratic programming for $z[k]$, defined as

$$\theta_k(\lambda[k]) = \begin{cases} D[k] + P^{\min}, & \frac{\lambda[k]}{2} < D[k] + P^{\min} \\ D[k] + P^{\max}, & D[k] + P^{\max} < \frac{\lambda[k]}{2} \\ \frac{\lambda[k]}{2}, & \text{otherwise.} \end{cases} \tag{8}$$

Next, for the second term in $g(\lambda)$, the subproblem

$$\begin{aligned} &\min_{u_i} \; \sigma_i \|u_i\|^2 + \lambda^\top u_i \\ &\text{s.t. } Au_i \le b_i \end{aligned} \tag{9}$$

has a strongly convex function over a convex set, which guarantees a unique solution, denoted by $\phi_i(\lambda)$. By substituting the expressions derived above, the dual problem becomes

$$\begin{aligned} &\max_{\lambda} \; g(\lambda) \\ &= \max_{\lambda} \left\{ \Theta(\lambda) + \sum_{i=1}^{N} \left(\sigma_i \|\phi_i(\lambda)\|^2 + \lambda^\top \phi_i(\lambda) \right) \right\}. \end{aligned} \tag{10}$$

Finally, the gradient ascent algorithm for (10) is derived using the gradient of $g(\lambda)$, which is verified in [12, Prop. 7.1.1]. The resulting algorithm is given by

$$\dot{\lambda} = \nabla g(\lambda) = -\theta(\lambda) + D + \sum_{i=1}^{N} \phi_i(\lambda) \tag{11}$$

where $\theta(\lambda)$ is a T-dimensional vector with components $\theta_k(\lambda[k])$. In the following, we demonstrate that an optimal solution of (6) can be obtained from (11).

Proposition 1. Suppose that the optimization problem (6) is feasible. Let Λ^* be the set of dual optimal solutions of the problem (10). Then, Λ^* is nonempty and we have $\lim_{t\to\infty} \lambda(t) = \lambda^*$ for some $\lambda^* \in \Lambda^*$ by the gradient ascent algorithm (11). Moreover, an optimal solution $u_i^* \in \mathbb{R}^T$ of the problem (6) satisfies

$$u_i^* = \phi_i(\lambda^*), \quad i \in \mathcal{N}. \tag{12}$$

Proof. In the primal problem (7), the objective function is convex and quadratic, the equality constraint (7b) is affine, and the sets $\mathcal{Z}$ and $\mathcal{U}$ are polyhedral. Thus, the primal problem (7) and the dual problem (10) have optimal solutions and there is no duality gap under feasible conditions [12, Prop. 6.2.2]. This implies that the set of dual optimal solutions Λ^* is nonempty. Therefore, based on the strong duality and the definition of $\phi_i(\lambda)$, it follows that an optimal solution u_i^* of the problem (6) is obtained from any dual optimal solution $\lambda^* \in \Lambda^*$, i.e., $u_i^* = \phi_i(\lambda^*)$.

Consider the gradient ascent algorithm (11) for the function $g(\lambda)$. Due to the concavity of $g(\lambda)$ [12], the algorithm converges to a dual optimal solution λ^* of (10), satisfying the optimality condition $\nabla g(\lambda^*) = 0_T$. ■

Note that the algorithm (11) requires the central aggregator, as illustrated in Fig. 1(a). In this semi-distributed framework, each EV solves its subproblem (9) in parallel, while exchanging the updated values with the aggregator running (11). In the next section, we will introduce a fully distributed setting in which the aggregator no longer needs a direct connection to each EV. Additionally, the algorithmic details for solving the subproblem (9) will be provided.

Remark 1. The proposed approach improves upon the dual-splitting method in [4], by reducing the size of communication vectors, thereby decreasing memory usage. This improvement is achieved through a reformulation of grid constraints with the variable z as in (7c) and obtaining a closed-form solution (as shown in (8)). In contrast, the

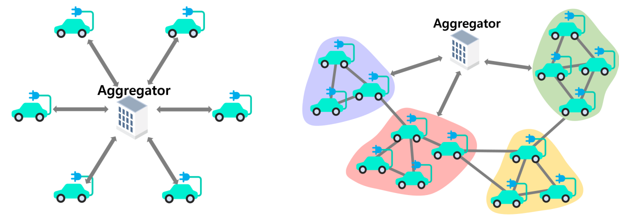

(a) semi-distributed (b) fully distributed

Fig. 1: Illustration of the communication network.

method in [4] requires $3T$-dimensional communication information, whereas our approach reduces this to T. □

IV. A Fully Distributed Solution

In this section, we propose a fully distributed, continuous-time algorithm for all EVs in a network to determine their optimal charging schedules for the optimization problem (6). The proposed algorithm leverages the blended dynamics approach [8]–[11], which is a useful tool to construct distributed optimization algorithms. Moreover, we introduce a Karush-Kuhn-Tucker (KKT) based algorithm for solving the problem (9), which is inspired by [13].

A. Preliminary: Blended Dynamics Theorem

This subsection briefly summarizes the result of [9], [10], tailored for a time-invariant system specified to our case. Consider the following heterogeneous multi-agent systems under diffusive output coupling as

$$\begin{aligned}\dot{x}_i &= h_i(x_i, y_i)\\ \dot{y}_i &= f_i(y_i, x_i) + \kappa \sum_{j\in\mathcal{N}_i} (y_j - y_i)\end{aligned} \tag{13}$$

for all $i \in \mathcal{N}$, where $x_i \in \mathbb{R}^m$ represents the private state which is not shared with other agents, $y_i \in \mathbb{R}^n$ represents the output communicated among agents, and κ is the coupling gain. The vector fields h_i and f_i are assumed to be globally Lipschitz with respect to x_i and y_i. The set of neighbors connected to agent i is denoted by $\mathcal{N}_i$. Under an undirected and connected graph, with a sufficiently large coupling gain κ, the synchronized behavior of the multi-agent systems (13) is characterized as

$$\begin{aligned}\dot{\hat{x}}_i &= h_i(\hat{x}_i, s), \quad i \in \mathcal{N}\\ \dot{s} &= \frac{1}{N}\sum_{i=1}^{N} f_i(s, \hat{x}_i)\end{aligned} \tag{14}$$

which is called the blended dynamics of (13). Given the stability of (14), the behavior of the multi-agent system (13) can be approximated by the blended dynamics (14) regardless of initial conditions. This is summarized as follows.

Lemma 1 ([10, Theorem 4])**.** Assume that there is a nonempty compact set $\mathscr{A}_b$ that is asymptotically stable for the blended dynamics (14). Let $\mathscr{D}_b \supset \mathscr{A}_b$ be an open subset of the domain of attraction of $\mathscr{A}_b$, and let

$$\begin{aligned}\mathscr{A}_x &:= \{[\hat{x}_1;\ldots;\hat{x}_N; 1_N \otimes s] : [\hat{x}_1;\ldots;\hat{x}_N; s] \in \mathscr{A}_b\},\\ \mathscr{D}_x &:= \{[\hat{x}_1;\ldots;\hat{x}_N; s_1;\ldots;s_N]\\ &\qquad : [\hat{x}_1;\ldots;\hat{x}_N; s] \in \mathscr{D}_b \text{ such that } \tfrac{1}{N}\textstyle\sum_{i=1}^{N} s_i = s\}.\end{aligned}$$

Then, for any compact set $K \subset \mathscr{D}_x$ and for any $\eta > 0$, there exists $\kappa^* > 0$ such that, for each $\kappa > \kappa^*$ and $[x_1(0);\ldots;x_N(0); y_1(0);\ldots;y_N(0)] \in K$, the solution to (13) exists for all $t \geq 0$, and satisfies

$$\limsup_{t\to\infty} \|[x_1(t);\ldots;x_N(t); y_1(t);\ldots;y_N(t)]\|_{\mathscr{A}_x} \leq \eta.$$

□

B. Proposed Fully Distributed Algorithm

We present a charging scheduling algorithm, utilizing the concept of blended dynamics to achieve a fully distributed solution. To this end, let us consider the aggregator as one of the agents, labeled as 0, which always participates in the network. We assume the entire communication graph, including the aggregator and EVs, is undirected and connected, as shown in Fig. 1(b). Agent 0 runs the following dynamics:

$$\dot{\lambda}_0 = -\theta(\lambda_0) + D + \kappa \sum_{j\in\mathcal{N}_0} (\lambda_j - \lambda_0) \tag{16}$$

while all the other agents of $i \in \mathcal{N}$ run

$$u_i = -\frac{1}{2\sigma_i}\left(\lambda_i + A^\top \nu_i\right) \tag{17a}$$

$$\dot{\nu}_i = -\nu_i + (\nu_i + A u_i - b_i)^+ \tag{17b}$$

$$\dot{\lambda}_i = u_i + \kappa \sum_{j\in\mathcal{N}_i} (\lambda_j - \lambda_i) \tag{17c}$$

where $\nu_i \in \mathbb{R}^{4T}$ is the private state, and $\lambda_i \in \mathbb{R}^T$ is a local version of λ, which is the only variable exchanged with its neighbors. Note that the proposed algorithm (16)–(17) is fully distributed, as each agent communicates its local variable λ_i with its neighbors. Since the overall network has $N+1$ agents, the blended dynamics of (16)–(17) becomes

$$\hat{u}_i = -\frac{1}{2\sigma_i}\left(s + A^\top \hat{\nu}_i\right) \tag{18a}$$

$$\dot{\hat{\nu}}_i = -\hat{\nu}_i + (\hat{\nu}_i + A\hat{u}_i - b_i)^+, \quad i \in \mathcal{N} \tag{18b}$$

$$\dot{s} = \frac{1}{N+1}\left(-\theta(s) + D + \sum_{i=1}^{N} \hat{u}_i\right) \tag{18c}$$

which is derived as (14). Here, (18c) is inspired by the gradient ascent algorithm (11) with the scaling of $1/(N+1)$, which can be compensated by scaling (16) and (17c).

Next, we explain that (18a) and (18b) are derived from the KKT conditions of the problem (9). To do this, we introduce the Lagrange multiplier $\hat{\nu}_i \in \mathbb{R}^{4T}$ for the inequality constraint of (9). Then, the dual problem is obtained as

$$\begin{aligned}&\max_{\hat{\nu}_i} \ \min_{u_i} \left(\sigma_i \|u_i\|^2 + \lambda^\top u_i + \hat{\nu}_i^\top (A u_i - b_i)\right)\\ &\text{s.t.} \ \ \hat{\nu}_i \geq 0_{4T}.\end{aligned} \tag{19}$$

Note that strong duality holds if the problem (9) is feasible with the affine constraint. For a given λ, the KKT conditions for the primal solution $\phi_i(\lambda)$ of (9) and the dual solution $\hat{\nu}_i^*(\lambda)$ of (19) are as follows:

$$\phi_i(\lambda) = -\frac{1}{2\sigma_i}\left(\lambda + A^\top \hat{\nu}_i^*(\lambda)\right) \quad \text{(stationarity)} \tag{20a}$$

$$\hat{\nu}_i^*(\lambda) = (\hat{\nu}_i^*(\lambda) + A\phi_i(\lambda) - b_i)^+. \tag{20b}$$

It is easy to verify that the expression (20b) is equivalent to $(\hat{\nu}_i^*(\lambda))^\top (A\phi_i(\lambda) - b_i) = 0$ (complementary slackness), $A\phi_i(\lambda) - b_i \leq 0$ (primal feasibility), and $\hat{\nu}_i^*(\lambda) \geq 0_{4T}$ (dual feasibility), as addressed in [13], [14]. As a result, equations (20a) and (20b) contribute to the design of the dynamics (18a) and (18b) (and hence (17a) and (17b)), respectively.

Remark 2. Each EV independently constructs its dynamics using only local information. This decentralized design is allowable because the aggregator holds global information, such as D, $P^{\min}$, and $P^{\max}$, which are included in θ of (16) as defined in (8). Unlike other distributed algorithms [4], [6], the proposed algorithm does not need prior knowledge of the total number of agents N, which can be difficult to obtain in a distributed way. Moreover, the algorithm ensures privacy by only exchanging the variable λ_i between agents. Each EV preserves its sensitive data such as charging schedule, energy demand, and battery degradation parameter. □

Now, the convergence of the proposed algorithm (16)–(17) will be analyzed in the remainder of this section. We first show the asymptotic stability of the blended dynamics (18).

Lemma 2. Suppose that the optimization problem (6) is feasible. Let Λ^* be the set of dual optimal solutions of the problem (10) and define

$$\Upsilon_i^* := \left\{ \hat{\nu}_i : \hat{\nu}_i = (\hat{\nu}_i + A u_i^* - b_i)^+ \right\}, \quad i \in \mathcal{N}$$

where $u_i^* \in \mathbb{R}^T$ is an optimal solution of (6). For any initial conditions, the trajectory $[\hat{\nu}_1(t); \ldots; \hat{\nu}_N(t); s(t)]$ associated with the blended dynamics (18) satisfies

$$\lim_{t\to\infty} \|[\hat{\nu}_1(t); \ldots; \hat{\nu}_N(t); s(t)]\|_{\mathscr{A}_b} = 0$$

where $\mathscr{A}_b$ is a compact subset of $\Upsilon_1^* \times \cdots \times \Upsilon_N^* \times \Lambda^*$.

Proof. See the Appendix. ■

We now have the main result of this paper. The following theorem states that the optimal solution u_i^* can be approximated by $u_i(t)$ with an arbitrarily small error when κ is large. We will use the same notation as in Lemma 2.

Theorem 1. Suppose that the optimization problem (6) is feasible. For any compact set $K \subset \mathbb{R}^{(5N+1)T}$ and for any $\eta > 0$, there exists $\kappa^* > 0$ such that, for each $\kappa > \kappa^*$ and $[\nu_1(0); \ldots; \nu_N(0); \lambda_0(0); \ldots; \lambda_N(0)] \in K$, the solutions to (16) and (17) satisfy

$$\limsup_{t\to\infty} \|[\nu_1(t); \ldots; \nu_N(t); \lambda_0(t); \ldots; \lambda_N(t)]\|_{\mathscr{A}_x} \le \eta \quad (21)$$

where

$$\mathscr{A}_x := \{[\nu_1; \ldots; \nu_N; 1_{N+1} \otimes s] : [\nu_1; \ldots; \nu_N; s] \in \mathscr{A}_b\}$$

and $\mathscr{A}_b$ is a compact subset of $\Upsilon_1^* \times \cdots \times \Upsilon_N^* \times \Lambda^*$.

Moreover, we have, for all $i \in \mathcal{N}$,

$$\limsup_{t\to\infty} \|u_i(t) - u_i^*\| \le \frac{\|A\|}{\underline{\sigma}} \eta$$

where $\underline{\sigma} := \min_{i \in \mathcal{N}} \sigma_i$.

Proof. For a given compact set K, we reconstruct the sets $\mathscr{D}_x$, $\mathscr{D}_b$, and $\mathscr{A}_b$ to apply Lemma 1 as follows. We define compact sets $K_\nu \subset \mathbb{R}^{4NT}$ and $K_s' \subset \mathbb{R}^{(N+1)T}$ satisfying $K \subset K_\nu \times K_s'$. There exists a bounded set

$$K_s = \left\{ s \in \mathbb{R}^T : s = \frac{1}{N+1} \sum_{i=0}^{N} s_i, \ [s_0; \ldots; s_N] \in K_s' \right\}.$$

Let $\mathscr{D}_b$ be an open and bounded set containing $K_\nu \times K_s$. By inspecting Lemma 2 and its proof, we find a nonempty compact set $\mathscr{A}_b$ where $\mathscr{D}_b$ is an open subset of its domain of attraction. By the construction, K is a compact subset of $\mathscr{D}_x$. Then, (21) immediately follows from Lemma 1.

Now we analyze the behavior of the trajectory of $u_i(t)$. From combining (12) with (20), we have $u_i^* = -(1/2\sigma_i)(\lambda^* + A^\top \nu_i^*)$ for any $\lambda^* \in \Lambda^*$ and $\nu_i^* \in \Upsilon_i^*$. Using this, we have, for all $i \in \mathcal{N}$,

$$\begin{aligned}
&\|u_i(t) - u_i^*\| \\
&= \inf_{\substack{\lambda^* \in \Lambda^* \\ \nu_i^* \in \Upsilon_i^*}} \left\| -\frac{1}{2\sigma_i}\big(\lambda_i(t) + A^\top \nu_i(t)\big) + \frac{1}{2\sigma_i}\big(\lambda^* + A^\top \nu_i^*\big) \right\| \\
&\le \inf_{\substack{\lambda^* \in \Lambda^* \\ \nu_i^* \in \Upsilon_i^*}} \frac{1}{2\underline{\sigma}} (\|\lambda_i(t) - \lambda^*\| + \|A\| \|\nu_i(t) - \nu_i^*\|) \\
&\le \frac{\|A\|}{\underline{\sigma}} \|[\lambda_0(t); \nu_1(t); \lambda_1(t); \ldots; \nu_N(t); \lambda_N(t)]\|_{\mathscr{A}_x}
\end{aligned}$$

where the last inequality comes from the fact that $\|A\| \ge 1$ and the definition of $\mathscr{A}_x$.

Therefore, we obtain, for all $i \in \mathcal{N}$ and $\kappa > \kappa^*$,

$$\limsup_{t\to\infty} \|u_i(t) - u_i^*\| \le \frac{\|A\|}{\underline{\sigma}} \eta$$

which completes the proof. ■

Remark 3. A notable feature of the proposed algorithm is its initialization-free nature, as demonstrated in Theorem 1. This allows for plug-and-play operation where EVs can freely join or leave the network while the algorithm is running, without resetting the initial conditions for the remaining agents. Then, the algorithm can adapt to real-time changes in operational conditions, as shown in Section V. □

Remark 4. We emphasize again that the proposed algorithm is designed to obtain the optimal solution $u_i^* \in \mathbb{R}^T$ for (6). While the solution $u_i(t)$ obtained from the algorithm approximates u_i^*, it may not be exact. However, with a sufficiently high κ, the solution's error can be made arbitrarily small. Additionally, we desire to achieve an exact solution asymptotically employing the proportional-integral protocol [11], [14], which is part of our future work. □

V. Simulation

This section provides numerical simulation to evaluate the effectiveness of the proposed algorithm (16)–(17). We consider EV scheduling over a day with hourly intervals, i.e., $T = 24$ and $\Delta T = 1$ hour. The base load D is scaled from real-world hourly load data from the Republic of Korea on April 1, 2023 [15]. All EVs have a 50 kWh battery capacity, with maximum discharging and charging powers of -5 kW and 5 kW, respectively. Energy capacity limits are set to 0 kWh and 50 kWh, with the initial energy level randomly set from 10% to 20%, and the reference energy level chosen between 25% and 35% of battery capacity. The battery degradation parameter σ_i is randomly set between 1 and 50. We choose the coupling gain $\kappa = 20$ for the

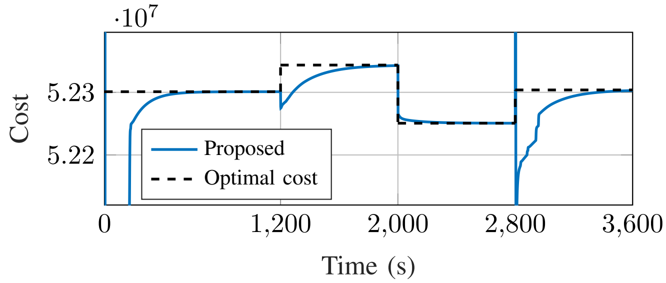

(a) Cost trajectory $J(u(t))$ and optimal cost J^*

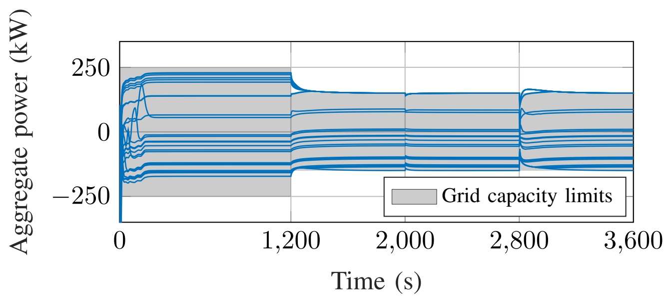

(b) The aggregate power trajectories $\{(\sum_{i=1}^N u_i[k])(t)\}_{k\in\mathcal{T}}$

Fig. 2: Trajectories of the proposed algorithm.

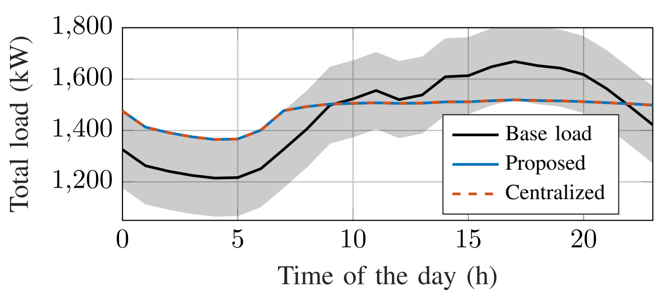

Fig. 3: Total load profile. The gray shaded area represents the allowable range by grid constraints, with upper and lower boundaries $D[k] + P^{\max}$ and $D[k] + P^{\min}$ for each $k \in \mathcal{T}$.

proposed algorithm (16)–(17). The forward Euler method of this algorithm is used for implementation, with a sampling time of 0.002 seconds.

We examine the following scenarios to demonstrate how the proposed algorithm works against the online changes of grid capacity limits and network topology:

S1) For $0 \le t < 1200$ s, the network consists of 50 EVs, with grid capacity limits of $P^{\max}, P^{\min} = \pm 250$ kW.

S2) At $t = 1200$ s, the grid capacity limits are changed to $P^{\max}, P^{\min} = \pm 150$ kW.

S3) At $t = 2000$ s, four EVs leave the network.

S4) At $t = 2800$ s, two new EVs join the network.

Simulation results are presented in Fig. 2 and Fig. 3. Fig. 2(a) shows the trajectory of the cost $J(u(t))$ from (6a) approximates the optimal cost J^* obtained by a centralized solver. In Fig. 2(b), each blue curve represents the trajectory of aggregated power $(\sum_{i=1}^N u_i[k])(t)$ for a given time slot $k \in \mathcal{T}$. A total of $T = 24$ curves are displayed. This demonstrates that the aggregated power eventually satisfies the grid capacity constraints. The solution $u_i(t)$ is obtained from the algorithm once $t = 3600$ s and is then applied for day-ahead scheduling. Using this solution, Fig. 3 compares the total load profile over a day with that obtained from the centralized solver, showing a close match while satisfying the grid capacity limits.

VI. Conclusion

In this paper, we propose a fully distributed EV scheduling algorithm that operates without requiring a central unit. By using the blended dynamics, the algorithm is initialization-free, enabling plug-and-play operation while preserving privacy. Our future work will focus on applying the algorithm in a receding horizon framework for real-world scenarios.

Appendix

A. Proof of Lemma 2 (Stability of the Blended Dynamics)

We first consider the following functions:

$$V_i^u = \sigma_i \|\hat{u}_i - u_i^*\|^2, \; V_i^\nu = \frac{1}{2}\|\nu_i - \nu_i^*\|^2, \quad i \in \mathcal{N},$$
$$V^s = \frac{N+1}{2}\|s - \lambda^*\|^2$$

where $\nu_i^* \in \Upsilon_i^*$ and $\lambda^* \in \Lambda^*$. Let us take the derivatives of V_i^u, V_i^ν, and V^s along (18). We have

$$\begin{aligned}
\dot{V}_i^u &= (\hat{u}_i - u_i^*)^\top \Big\{ -A^\top \Big(-\hat{\nu}_i + (\hat{\nu}_i + A\hat{u}_i - b_i)^+ \Big) \\
&\quad + \frac{1}{N+1}\Big(\theta(s) - D - \sum_{i=1}^N \hat{u}_i \Big) \Big\} \\
&= -2\sigma_i \|\hat{u}_i - u_i^*\|^2 - (\hat{u}_i - u_i^*)^\top (s - \lambda^*) \\
&\quad - (\hat{u}_i - u_i^*)^\top A^\top \Big((\hat{\nu}_i + A\hat{u}_i - b_i)^+ - \nu_i^* \Big) \\
&\quad + \frac{1}{N+1}\Big\{ (\hat{u}_i - u_i^*)^\top (\theta(s) - \theta(\lambda^*)) \\
&\quad - (\hat{u}_i - u_i^*)^\top \Big(\sum_{i=1}^N \hat{u}_i - \sum_{i=1}^N u_i^* \Big) \Big\}.
\end{aligned}$$

For this, one uses $\hat{u}_i = -(1/2\sigma_i)(s + A^\top \hat{\nu}_i)$ (similarly, $u_i^* = -(1/2\sigma_i)(\lambda^* + A^\top \nu_i^*)$) and $\theta(\lambda^*) = D + \sum_{i=1}^N u_i^*$, as derived from (20) and Proposition 1. Next,

$$\begin{aligned}
\dot{V}_i^\nu &= (\hat{\nu}_i - \nu_i^*)^\top \Big(-\hat{\nu}_i + (\hat{\nu}_i + A\hat{u}_i - b_i)^+ \Big) \\
&= -\Big\| \hat{\nu}_i - (\hat{\nu}_i + A\hat{u}_i - b_i)^+ \Big\|^2 \\
&\quad - \Big(\hat{\nu}_i - (\hat{\nu}_i + A\hat{u}_i - b_i)^+ \Big)^\top \Big((\hat{\nu}_i + A\hat{u}_i - b_i)^+ - \nu_i^* \Big) \\
&\le -\Big\| \hat{\nu}_i - (\hat{\nu}_i + A\hat{u}_i - b_i)^+ \Big\|^2 \\
&\quad - (A\hat{u}_i - b_i)^\top \big(\nu_i^* - (\hat{\nu}_i + A\hat{u}_i - b_i)^+ \big).
\end{aligned}$$

To derive the second equality, adding and subtracting $(\hat{\nu}_i + A\hat{u}_i - b_i)^+$ to $(\hat{\nu}_i - \nu_i^*)$ may be helpful. For the last inequality, we apply the following inequality obtained from the property of the max operator[1], that is,

$$-\left(\hat{\nu}_i - (\hat{\nu}_i + A\hat{u}_i - b_i)^+\right)^\top \left((\hat{\nu}_i + A\hat{u}_i - b_i)^+ - \nu_i^*\right) \\ \leq -\left(A\hat{u}_i - b_i\right)^\top \left(\nu_i^* - (\hat{\nu}_i + A\hat{u}_i - b_i)^+\right).$$

We also have

$$\dot{V}^s = (s - \lambda^*)^\top \left(-\theta(s) + D + \sum_{i=1}^N \hat{u}_i \right)$$
$$= (s - \lambda^*)^\top \left(\sum_{i=1}^N \hat{u}_i - \sum_{i=1}^N u_i^* \right) - (s - \lambda^*)^\top (\theta(s) - \theta(\lambda^*))$$

using $\theta(\lambda^*) = D + \sum_{i=1}^N u_i^*$ again.

Now we consider the Lyapunov function candidate $V := \sum_{i=1}^N (V_i^u + V_i^\nu) + V^s$. Note that

$$\begin{aligned} &-(\hat{u}_i - u_i^*)^\top A^\top \left((\hat{\nu}_i + A\hat{u}_i - b_i)^+ - \nu_i^*\right) \\ &\quad - (A\hat{u}_i - b_i)^\top \left(\nu_i^* - (\hat{\nu}_i + A\hat{u}_i - b_i)^+\right) \\ &= \left((\hat{\nu}_i + A\hat{u}_i - b_i)^+\right)^\top (Au_i^* - b_i) - (\nu_i^*)^\top (Au_i^* - b_i) \\ &= \left((\hat{\nu}_i + A\hat{u}_i - b_i)^+\right)^\top (Au_i^* - b_i) \leq 0 \end{aligned}$$

where we use the complementary slackness and primal feasibility of the KKT conditions, as discussed below (20b). With this in mind, taking the derivative of V along (18) gives

$$\begin{aligned} \dot{V} \leq &- \sum_{i=1}^N 2\sigma_i \|\hat{u}_i - u_i^*\|^2 - \sum_{i=1}^N \left\|\hat{\nu}_i - (\hat{\nu}_i + A\hat{u}_i - b_i)^+\right\|^2 \\ &- \frac{N}{N+1}(s - \lambda^*)^\top (\theta(s) - \theta(\lambda^*)) \\ &- \frac{1}{N+1}\Big\{(s - \lambda^*)^\top (\theta(s) - \theta(\lambda^*)) \\ &\quad - (w - w^*)^\top (\theta(s) - \theta(\lambda^*)) + (w - w^*)^\top (w - w^*)\Big\} \end{aligned}$$

where $w := \sum_{i=1}^N \hat{u}_i$ and $w^* := \sum_{i=1}^N u_i^*$. From the component-wise non-decreasing property of θ (which can be verified from (8)), we have $(s - \lambda^*)^\top (\theta(s) - \theta(\lambda^*)) \geq 0$. In the remaining, we assert that the last term enclosed in braces is also non-negative. Within this proof, each component of T-dimensional vectors is denoted with an index k. For $k \in \mathcal{T}$, if $|\theta_k(s[k]) - \theta_k(\lambda^*[k])| \leq |w[k] - w^*[k]|$, then $(w[k] - w^*[k])^2 - (w[k] - w^*[k])(\theta_k(s[k]) + \theta_k(\lambda^*[k])) \geq 0$. Otherwise, we show that $(\theta_k(s[k]) - \theta_k(\lambda^*[k]))(s[k] - \lambda^*[k] - w[k] + w^*[k]) \geq 0$ holds. For the case where $s[k] \leq \lambda^*[k]$, we have $(\theta_k(s[k]) - \theta_k(\lambda^*[k])) \leq 0$ from the non-decreasing property of θ_k. Therefore,

$$s[k] - \lambda^*[k] - w[k] + w^*[k] \\ < s[k] - \lambda^*[k] + \theta_k(s[k]) - \theta_k(\lambda^*[k]) \leq 0.$$

The proof for the case where $s[k] > \lambda^*[k]$ is analogous, hence omitted. By combining all these facts, we conclude that $\dot{V} \leq 0$.

[1]For any $x \in \mathbb{R}^n$ and $y \in \mathbb{R}_+^n$, $\left((x)^+ - x\right)^\top \left(y - (x)^+\right) \geq 0$. Let $x = \hat{\nu}_i + A\hat{u}_i - b_i$ and $y = \nu_i^*$.

Since V is positive definite and radially unbounded, the solution of (18) is bounded. By LaSalle's invariance principle [16], it is guaranteed that the trajectory $[\hat{\nu}_1(t); \ldots; \hat{\nu}_N(t); s(t)]$ converges to the set such that $\dot{V} = 0$ whose component satisfies that $\hat{u}_i = u_i^*$, $\hat{\nu}_i = (\hat{\nu}_i + A\hat{u}_i - b_i)^+$, and $\theta(s) = \theta(\lambda^*)$. In other words, the trajectory converges to $\Upsilon_1^* \times \cdots \times \Upsilon_N^* \times \Lambda^*$. Consequently, the bounded solution converges to the compact subset of $\Upsilon_1^* \times \cdots \times \Upsilon_N^* \times \Lambda^*$ denoted by $\mathscr{A}_b$. This completes the proof.

References

[1] M. Yilmaz and P. T. Krein, "Review of the impact of vehicle-to-grid technologies on distribution systems and utility interfaces," *IEEE Trans. Power Electronics*, vol. 28, no. 12, pp. 5673–5689, 2012.

[2] Q. Wang, X. Liu, J. Du, and F. Kong, "Smart charging for electric vehicles: A survey from the algorithmic perspective," *IEEE Communications Surveys & Tutorials*, vol. 18, no. 2, pp. 1500–1517, 2016.

[3] E. Sortomme, M. Hindi, S. MacPherson, and S. Venkata, "Coordinated charging of plug-in hybrid electric vehicles to minimize distribution system losses," *IEEE Trans. Smart Grid*, vol. 2, no. 1, pp. 198–205, 2011.

[4] C. L. Floch, F. Belletti, and S. Moura, "Optimal charging of electric vehicles for load shaping: A dual-splitting framework with explicit convergence bounds," *IEEE Trans. Transportation Electrification*, vol. 2, no. 2, pp. 190–199, 2016.

[5] J. Riversa, C. Goebel, and H. A. Jacobsen, "Distributed convex optimization for electric vehicle aggregators," *IEEE Trans. Smart Grid*, vol. 8, no. 4, pp. 1852–1863, 2016.

[6] A. Falsone, I. Notarnicola, G. Notarstefano, and M. Prandini, "Tracking-ADMM for distributed constraint-coupled optimization," *Automatica*, vol. 117, no. 108962, 2020.

[7] N. Rahbari-Asr, M.-Y. Chow, J. Chen, and R. Deng, "Distributed real-time pricing control for large-scale unidirectional V2G with multiple energy suppliers," *IEEE Trans. Industrial Informatics*, vol. 12, no. 5, pp. 1953–1962, 2016.

[8] J. Kim, J. Yang, H. Shim, J.-S. Kim, and J. H. Seo, "Robustness of synchronization of heterogeneous agents by strong coupling and a large number of agent," *IEEE Trans. Automatic Control*, vol. 61, no. 10, pp. 3096–3102, 2016.

[9] J. G. Lee and H. Shim, "A tool for analysis and synthesis of heterogeneous multi-agent systems under rank-deficient coupling," *Automatica*, vol. 117, no. 108952, 2020.

[10] J. G. Lee and H. Shim, "Design of heterogeneous multi-agent system for distributed computation," In: Jian ZP., Prieur C., Astolfi A. (eds) *Trends in Nonlinear and Adaptive Control*. Lecture Notes in Control and Information Sciences, vol. 488, pp. 83–108, Springer, 2022.

[11] S. Lee and H. Shim, "Blended dynamics approach to distributed optimization: Sum convexity and convergence rate," *Automatica*, vol. 141, no. 110290, 2022.

[12] D. P. Bertsekas, *Nonlinear Programming*, 3rd ed., Athena Scientific, 2016.

[13] Y. Zhu, W. Yu, G. Wen, G. Chen, and W. Ren, "Continuous-time distributed subgradient algorithm for convex optimization with general constraints," *IEEE Trans. Automatic Control*, vol. 64, no. 4, pp. 1694–1701, 2018.

[14] S. Yang, Q. Liu, and J. Wang, "A multi-agent system with a proportional-integral protocol for distributed constrained optimization," *IEEE Trans. Automatic Control*, vol. 62, no. 7, pp. 3461–3467, 2017.

[15] *Load data of the Republic of Korea*, Electric Power Statistics Information System, April 1, 2023. [Online]. Available: https://epsis.kpx.or.kr/epsisnew/selectEkgeEpsMepRealChart.do.

[16] H. K. Khalil, *Nonlinear Systems*, 3rd ed., Prentice-Hall, 2002.